ISSN: 3068-014X

Research Article

Archivos de Ciencia e Investigación

Comparative Study of Decentralized Grid-Forming Converter Controls for Inverter-Based Microgrids

Fadi Kelada[1], Jerome Buire[1*] and Nouredine HadjSaid[2]

[1]*University of Grenoble Alpes, CNRS, Grenoble INP, France*

[2]*Nanyang Technological University, Singapore*

[*]Corresponding Author
Jerome Buire, University of Grenoble Alpes, CNRS, Grenoble INP, France.

Submitted: 2025, Aug 04; **Accepted:** 2025, Sep 08; **Published:** 2025, Sep 11

Citation: Kelada, F., Buire, J., Hadjsaid, N. (2025). Comparative Study of Decentralized Grid-Forming Converter Controls for Inverter-Based Microgrids. *Arch Cienc Investig, 1*(2), 01-06.

Abstract

With the heavy integration of Inverter-based Resources (IBR) into the different levels of the electrical network, they are gradually requested to replace the conventional Synchronous Machines (SM) in maintaining the network voltage and frequency references. Such Grid-forming (GFM) controllers recently reported in literature include conventional Droop control, nonlinear oscillator-based controls, namely the dispatchable Virtual Oscillator Control (dVOC), Synchroverter and Matching controls. This article aims to reveal the underlying resemblance between these grid-forming controls and the conventional Droopbased strategies being the most commonly used in the decentralized and hierarchical control of Microgrids (MGs). Based on the derived similarities in their dynamics, tuning the different controllers' parameters to achieve equivalent transient and steady state dynamics maintaining P-f and Q-V relations is deduced and validated using time domain simulations.

Keywords: Decentralized Control, Grid-forming Converter Controls, Inverter-Dominated Networks, Microgrids, Tuning of Grid-Forming Power Controllers

1. Introduction

Stability and resilience of the electrical power networks is the uttermost priority of the network operators. These cornerstone characteristics of the power systems have been maintained all over the years by huge generation plants that were traditionally dominated by Synchronous Machines (SM) of gigantic inertia reservoir and well-established electromechanical interactions aintaining the synchronization and stiffness of the network. Lately with the gradual retraction of SMs, power converters interfacing IBRs are slowly taking over the role of maintaining this synchronization and stiffness of the network by forming themselves the voltage magnitude and frequency references [1].

In that sense, many grid-forming control strategies are being reported in literature. Droop-based primary control–and its variants–is the most commonly used grid-forming control in networks with parallel operation of inverters such as MGs. This is due to many obvious reasons, such as ease of implementation, resemblance to conventional SMs' primary control and decentralized power sharing capabilities [2-5]. The recent research on grid-forming controls for voltage source converters presents other novel strategies to control the converters in a grid-forming manner as explained above [6,7]. A wide range of such inverter controls proposed in literature are called the Virtual Synchronous Generator (VSG).

These controllers emulate some of the SMs' dynamics to generate the control signals for the converters [1,7]. Others match the converters' dynamics to that of SMs and prove that the DC-link capacitor voltage dynamics are analogous to the rotational speed in SMs and thus can be utilized to mimic SMs' synchronization with the grid in what is called the Matching control [8]. Others relied on modelling converters as coupled oscillators and define a control law to synchronize such oscillators using consensus-like dynamics as with the case of Virtual Oscillator Control (VOC) and its dispatchable variant the (dVOC) [9].

The vast majority of these grid-forming controllers deduce the frequency information from the active power imbalance and similarly with the voltage reference signal using knowledge of the reactive power change to maintain parallel loadsharing with other parallel units. In this article, a comparative analysis of these P-f and Q-V dynamics in the previously mentioned GFM controls is carried out and resemblance to the conventional droop functions are highlighted. The contribution of this paper is thus twofold, first by putting the P-f and QV dynamics of the different GFM controllers in the same canonical form, their steady state and

transient behavior is proved to be nearly identical by manipulating their different tuning parameters. Second, with that in hand, an equivalent tuning criterion to achieve a certain required behavior by the user is proposed.

2. Grid-Forming Control Strategies Overview

One of the most frequent control topologies of VSC converters is the cascaded control in dq0-reference frame, in which the inner loops voltage reference (e*dq0) and the rotational frame angle (θ) is generated by the outer power module where all the GFM controllers–which will be presented here– are applied [6,7,10]. This VSC control topology is the one considered here as shown in Figure 1.

2.1 Droop-Based Control

As mentioned before, there exist many variants of the droop control, however, they all share the same basic concept which is to emulate Synchronous Machines' P-f and Q-V control behavior of decreasing frequency as active power increases or vice-versa. It was first used in microgrids for parallel operation of Uninterruptible Power Supplies (UPS) for its plug-and play and reliable power sharing capabilities. The droop functions considered here are shown in Figure 2 [11]. They can be expressed in time domain as follows:

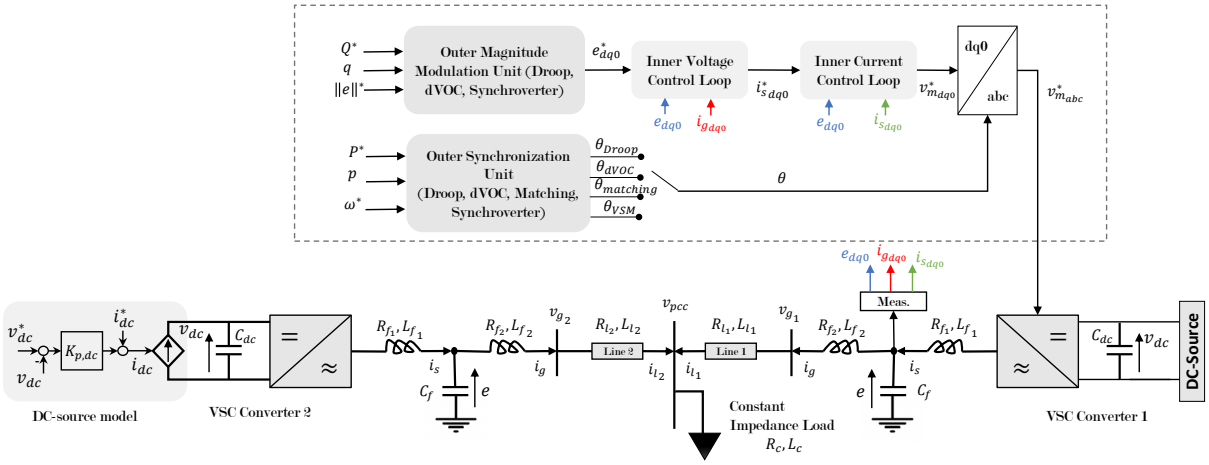

Figure 1: Simulated Network and Control Topology

$$\frac{1}{m_p.\omega_f}\frac{d\delta\omega}{dt} = P^* - p - \frac{1}{m_p}.\delta\omega \qquad (1)$$

$$\frac{1}{n_q.\omega_f}\frac{d\delta E}{dt} = Q^* - q - \frac{1}{n_q}.\delta E \qquad (2)$$

where $\delta\omega = \omega - \omega^*$ and $\delta E = e_{dq0} - \|e\|^*$. m_p and n_q are respectively the P-f and Q-V droop coefficients, ω_f is the measurements' filter cut-off frequency and $\|e\|^*$ is the voltage reference magnitude.

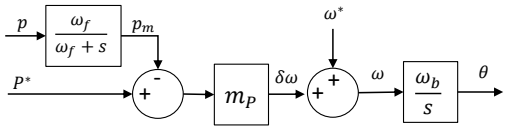

(a) P-f Droop

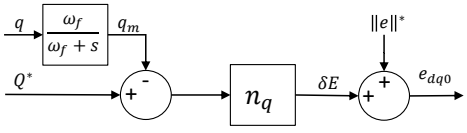

(b) Q-V Droop

Figure 2: Conventional Droop Functions

2.2 Synchroverter Control

The grid-connected power converters which emulate the steady-state and transient characteristics of Synchronous Generators (SG) are called Virtual Synchronous Generators (VSG). There exist different versions of the VSG scheme that differ according to the level of detail and the captured dynamics. However, one VSG version which captures the main SG dynamics without the complexity of SG full order models is the synchroverter model. All the properties of SG can be emulated in the synchroverter control with the advantage of being tunable even in real time operation [12]. The synchroverter upper frequency drooping loop and lower voltage drooping loop shown in Figures 3 & 4 can be reduced to the following form in time domain:

$$J\omega^*.\frac{d\omega}{dt} = P^* - p - D_p\omega^*.\delta\omega \qquad (3)$$

$$K.\frac{d\varphi}{dt} = Q^* - q - D_q.\delta E \qquad (4)$$

where $\delta E = (\|e\| - \|e\|^*)$, $\|e\|$ is the measured voltage magnitude at the output filter. D_p, J are the virtual damping and moment of inertia of the rotor respectively and D_q, K are the voltage drooping coefficient and an integrator gain respectively.

Despite the very close resemblance between (1)-(2) and (3)- (4), it should be underlined that D_q in Figures 3 & 4 plays the role of an outer voltage proportional controller which may interact with the

inner voltage control of the cascaded structure. The time constant τ_v of this outer voltage loop can be estimated as $\tau_v \approx K/D_q$ [12]. This τv should be sufficiently slower than the inner voltage loop to avoid any interaction.

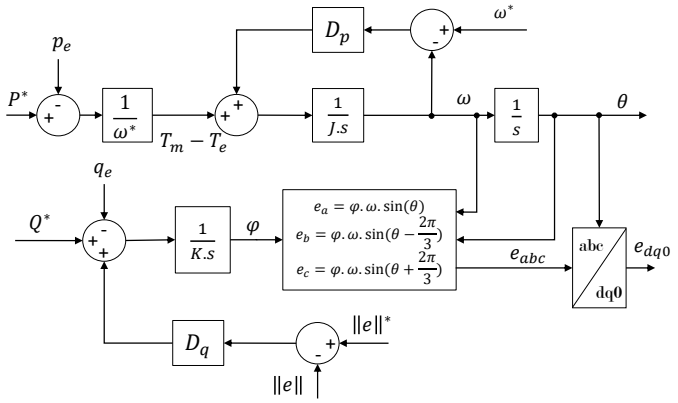

Figure 3: Synchroverter Controller

2.3 Dispatchable Virtual Oscillator Control (dVOC)

Faster time-domain controllers based on synchronization of coupled nonlinear oscillators are proposed by the Virtual Oscillator Control (VOC) and its modified version with dispatchable active power injections and voltage setpoints (dVOC) [9,13,14]. The original VOC version relied on controlling inverters to behave like virtual Liénard-type oscillators but it was not dispatchable i.e., track references of power injections and voltage references thus was not suitable as a GFM-converter strategy [9,13]. Its dispatchable version (dVOC) proposed in, and presented here (Figure 4) offers a combination of synchronizing feedback and a decentralized magnitude control law for a global phase and magnitude synchronization of coupled oscillators, with respect to setpoints of phase shift, frequency and magnitude [14].

The aforementioned properties of this controller are achieved through a decentralized control law which–through local measurement–synchronize the network of oscillators by acting on the magnitude and angle of their oscillations represented here by the voltage $e_i = R(\theta_i)(\|e_i\|, 0)$. This control law is expressed as follows [7,9]:

$$\frac{d}{dt}e_i = \omega_0 J e_i + \eta\Big(\underbrace{K_i e_i - R(\kappa) i_{s,i}}_{\text{Phase error } \varepsilon_{\theta,i}(e_i, i_{s,i})} + \underbrace{\alpha\phi_i(e_i)e_i}_{\text{Magnitude error } \varepsilon_{v,i}(e_i)}\Big) \quad (5)$$

where $i_{s,i}$ is the measurement of the output current of the converter, ω_0 is the nominal grid frequency, the matrix

$$R(\circ) := \begin{bmatrix} \cos(\circ) & -\sin(\circ) \\ \sin(\circ) & \cos(\circ) \end{bmatrix}$$

is a 2D rotation matrix, $J := R(\pi/2)$,

$$K_i := \frac{1}{e_i^{*2}} R(\kappa).\begin{bmatrix} P_i^* & Q_i^* \\ -Q_i^* & P_i^* \end{bmatrix}, \quad \phi_i(e_i) := \frac{\|e_i\|^{*2} - \|e_i\|^2}{\|e_i\|^{*2}}$$

$\omega_0 J e_i$ is the standard equation of a harmonic oscillator in rectangular coordinates. The quantities $\eta > 0$ and $\alpha > 0$ are the synchronization and voltage amplitude regulation gains respectively. The parameter $\kappa \in [0, \pi]$ can be used to adjust the controller to adapt to the line parameters such that $\kappa = \tan{-1}(X_i/R_i)$. $\kappa = 0$ corresponds to pure resistive lines and $\kappa = \pi/2$ corresponds to pure inductive lines.

P^*_i, Q^*_i and $\|ei\|^*$ are the active power, reactive power, and voltage magnitude setpoints respectively. $\phi_i(e_i)$ is the normalized quadratic voltage error, which can be interpreted as a voltage regulator, i.e., depending on its sign, the voltage vector e_i can be scaled up or down.

According to the definition of synchronization of coupled oscillators [9], the synchronization is achieved when the phase error term $\varepsilon_{\theta,i}$ and the magnitude error term $\varepsilon_{v,i}$ shown in (5) are eliminated, i.e., the N-coupled oscillators now have the same magnitude and phase and rotate with the same synchronization frequency ω_0.

For comparison purpose, to keep the P-f and Q-V relations as shown previously in the droop and synchroverter equations, $\kappa = \pi/2$ is assumed. This results in the dVOC control law in (5) being reformulated into (cf. proposition 4 in [9]):

$$\frac{d\theta_i}{dt} = \omega_0 + \eta\left(\frac{P_i^*}{\|e_i\|^{*2}} - \frac{p_i}{\|e_i\|^2}\right) \quad (6)$$

$$\frac{d\|e_i\|}{dt} = \eta\left(\frac{Q_i^*}{\|e_i\|^{*2}} - \frac{q_i}{\|e_i\|^2}\right)\|e_i\| + \frac{\eta\alpha}{\|e_i\|^{*2}}\left(\|e_i\|^{*2} - \|e_i\|^2\right)\|e_i\| \quad (7)$$

To account for the measurements' filter added, and assuming $\|\dot{e}_i\| \approx 0$ and $1/\|e_i\|^{*2} \approx 1/\|e_i\|^2$ (thanks to the inner voltage control loop), (6) and (7) are reformulated in time domain as:

$$\frac{\|e\|^{*2}}{\eta.\omega_f}\frac{d\delta\omega}{dt} = P^* - p - \frac{\|e\|^{*2}}{\eta}.\delta\omega \quad (8)$$

$$\frac{2\alpha\|e\|^*}{\omega_f}\frac{d\delta E}{dt} = Q^* - q - 2\alpha\|e\|^*.\delta E \quad (9)$$

where $\delta\omega = \omega - \omega_0$ and $\delta E = \|e\| - \|e\|^*$

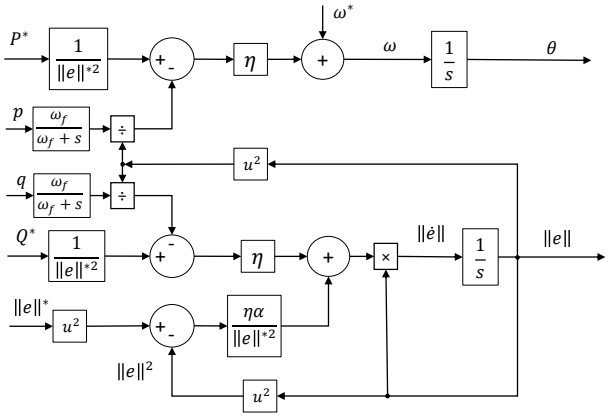

Figure 4: dVOC Controller

2.4 Matching Control

Another analogous control to VSG, is the matching control, which is designed to assure that the closed-loop dynamics of the converter exactly match that of SMs, in the sense that the DC-link capacitor voltage serves as the key control and imbalance signal in a similar fashion as is SM's rotational speed is an indication of equilibrium between generation and consumption. The objective of this control is thus to mimic the SG's synchronization with the grid through mimicking its electromechanical interactions [8,15].

In order to incorporate these dynamics in the control, the angle dynamics of the matching control can be obtained by dynamic feedback of the measured DC voltage as shown in (10) [8], or expressed in relative coordinates as in (11) [7].

$$\omega = \gamma . v_{dc} \tag{10}$$

$$\omega - \omega_0 = K_\theta (v_{dc} - v_{dc}^*) \tag{11}$$

where the constant $\gamma = \omega_0 / v^*_{dc} > 0$ encodes the ratio between the nominal AC frequency ω_0 and the DC reference voltage v^*_{dc}, and $K_\theta > 0$ is a gain to be tuned.

Assuming a P-controller to control the DC-link capacitor voltage (cf. Figure 1) such that:

$$i_{dc} - i_{dc}^* = K_{p,dc} . (v_{dc}^* - v_{dc}) \tag{12}$$

Substituting by (12) in (11) and exchanging i_{dc} by p/vdc and i^*_{dc} by P^*/v^*_{dc} we get:

$$\omega - \omega_0 = \frac{K_\theta}{K_{p,dc} . v_{dc}^*} (P^* - p) \tag{13}$$

Finally, considering the low-pass filter effect (cf. Fig. 5), we can express the matching control dynamics in time domain as:

$$\frac{v_{dc}^* K_{p,dc}}{\omega_f K_\theta} \frac{d\delta\omega}{dt} = P^* - p - \frac{v_{dc}^* K_{p,dc}}{K_\theta} . \delta\omega \tag{14}$$

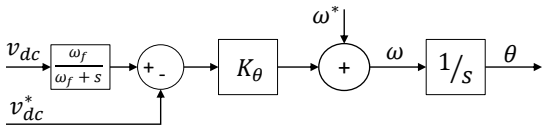

Figure 5: Matching Controller

3. Uncovering the Underlying Dynamics

The information on how each controller deduces the rotational electrical frequency (ω) from the change in active power can be concluded from (1), (3), (8) and (14) and is summarized in Table I to highlight the equivalences in dynamics. Similarly, the information on how each controller computes the reference voltage magnitude for the inner control loops from the reactive power imbalance information can be deduced from (2), (4) and (9) and summarized in Table I.

	P-f Dynamics					Q-V Dynamics				
	Transient Term				S.S. Term	Transient Term				S.S. Term
Droop	$\frac{1}{m_p \omega_f}$	$\frac{d\delta\omega}{dt} =$	P^*	$-p$	$-\frac{1}{m_p}\ \delta\omega$	$\frac{1}{n_q \omega_f}$	$\frac{d\delta E}{dt} =$	Q^*	$-q$	$-\frac{1}{n_q}\ \delta E$
VSM	$J\omega^*$	$\frac{d\omega}{dt} =$	P^*	$-p$	$-D_p\omega^*\ \delta\omega$	K	$\frac{d\varphi}{dt} =$	Q^*	$-q$	$-D_q\ \delta E$
dVOC	$\frac{\|e\|^{*2}}{\eta\omega_f}$	$\frac{d\delta\omega}{dt} =$	P^*	$-p$	$-\frac{\|e\|^{*2}}{\eta}\ \delta\omega$	$\frac{2\alpha\|e\|^*}{\omega_f}$	$\frac{d\delta E}{dt} =$	Q^*	$-q$	$-\frac{\|e\|^{*2}}{\eta}\ \delta E$
Match.	$\frac{v_{dc}^* K_{p,dc}}{\omega_f K_\theta}$	$\frac{d\delta\omega}{dt} =$	P^*	$-p$	$-\frac{v_{dc}^* K_{p,dc}}{K_\theta}\ \delta\omega$					

Table 1: Summary

Comparing these P-f dynamics with the well-known SMs'swing equation shown in (15), we can deduce by identification the terms incorporating the controllers' tuning parameters relative to the inertia constant (H), which in other words, define mathematically how the frequency signal's rate of change will be in case there is an imbalance in the active power. We can also deduce the terms relative to the frictional damping (D) which in this context represents the steady state error in the frequency signal from the primary control.

$$2H\frac{d\delta\omega}{dt} = P_m - P_e - D.\delta\omega \qquad (15)$$

It is clear how the choice of the measurements' filter cut-off frequency ω_f affects the transient rate of change of the frequency. Lower values of the cut-off frequency is usually required to achieve good attenuation of high frequency distortion components in the measured quantities and avoid any interactions with inner control loops [11]. This will directly solve the issue with the synchroverter's outer voltage regulation time constant τ_v also since $\tau_v \approx 1/\omega_f$.

By choosing the suitable filter cut-off frequency and since the droop coefficients are easy to set from relations (16), one can tune by identification all the other controllers' parameters as summarized in the upper third of Table II. This tuning criteria thus sets the required transient and steady state behavior of the frequency and voltage output signals by tuning the transient and steady state terms as marked in Table I.

$$m_p = \frac{\Delta\omega}{\Delta P}, \quad n_q = \frac{\Delta V}{\Delta Q} \qquad (16)$$

To test and validate the previous claims, the four controllers compared in this paper are implemented in the upper power controller modules of a classic cascaded controlled voltage source converter as previously mentioned. The test network consists of two 10 kVA, 400V (RMS phase-to-phase) VSC converters each connected in parallel through a line to a 10 kW (pure resistive) constant impedance load (≡ 14.52Ω per phase) as shown in Figure 1. A load step increase of +0.33 p.uis simulated at t=1.5s and decreased back to normal again at t=2.5s to compare the P-f and Q-V dynamics of the different controllers. The equivalent tuning of the different controllers' parameters according to the established criteria and equivalent dynamic equations is shown in Table II.

Controller	Tuning Parameter Equivalent	Controller	Tuning Parameter Equivalent
Droop	$m_p = {}^{\Delta\omega}/_{\Delta P}$	Matching	$K_\theta = m_p.K_{p,dc}.v_{dc}^*$
	$n_q = {}^{\Delta V}/_{\Delta Q}$		—
dVOC	$\eta = m_p.\|\|e\|\|^{*2}$	VSM	$D_p = {}^{1}/_{m_p.\omega_b}$, $J = {}^{1}/_{m_p.\omega_b.\omega_f}$
	$\alpha = {}^{1}/_{2n_q\|\|e\|\|^*}$		$D_q = {}^{1}/_{n_q}$, $K = {}^{1}/_{n_q.\omega_f}$
Cascaded Current/Voltage Controllers (in p.u)			
$K_{p_{VL}} = 0.4744$	$K_{i_{VL}} = 51$	$K_{p_{CL}} = 0.5394$	$K_{i_{CL}} = 586.9$
Droop Controller			
$m_p = 1.5708 \times 10^{-4}$ (0.5%)	$n_q = 6.667 \times 10^{-5}$ (0.1%)		$\omega_f = 0.05\omega_b$
Virtual Synchronous Machine (VSM)			
$D_p = 20.264$	$J = 1.2901$	$D_q = 15 \times 10^3$	$K = 954.88$
Dispatchable Virtual Oscillator Control (dVOC)			
$\eta = 25.1327$	$\alpha = 18.75$		$\|\|e\|\|^* = 400V$
Matching Control			
$K_\theta = 0.1885$	$K_{p_{dc}} = 1.5$		$v_{dc}^* = 800V$
Lines Parameters			
$R_{l1}/X_{l1} = 2.3$		$R_{l2}/X_{l2} = 0.6$	

Table 2: Network and VSCs' Control Parameters

Figures 6a, 6b show the active power supplied by the first converter and the deduced frequency signal respectively. It could be noticed how the rate of change of frequency (ROCOF) as well as the steady state frequency value is quasi-identical by all the different controllers which validates the previously derived P-f dynamic equations and the respective tuning in steering the P-f dynamics to behave in a controlled and droop-equivalent manner. In a similar fashion, Figures 6c,6d show the reactive power supplied by the same converter and the measured voltage magnitude at the capacitor filter. Again, quasi-identical voltage and reactive power dynamics are spotted which validates by its turn the aforementioned proposed equivalence of the Q-V dynamics between the different controllers and the validity of the tuning criteria in controlling the Q-V behavior according to user preferences.

This configuration and results were tested in a wide range of the feasible values of the droop coefficients while respecting the same tuning method and again the same conclusions were obtained. On the other hand, choosing other non-equivalent values for the tuning parameter, each controller starts to behave differently

and the quasi-identical dynamics start to deviate. Which further validates the analysis conducted here.

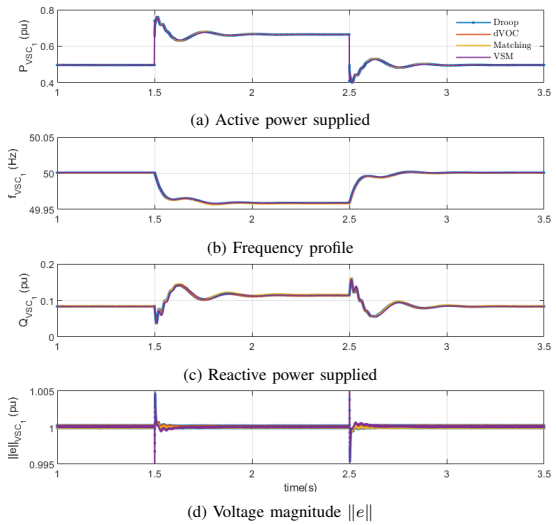

(a) Active power supplied

(b) Frequency profile

(c) Reactive power supplied

(d) Voltage magnitude $\|e\|$

Figure 6: VSC Converter 1 Response to the Load Step at t=1.5-2.5s

4. Conclusions

In this article the embedded droop-like dynamics of the four major grid-forming controllers proposed for VSCs in literature, namely the Droop, dVOC, Synchroverter and Matching are compared and the underlying equivalences are highlighted and then utilized to achieve equivalent tuning of the controllers' dynamics to obtain equivalent P-f and Q-V relationships. It could be deduced how–regardless of the different control architecture and different tuning parameters–they can all be reduced to the very similar dynamics and thus by identification their different parameters can be tuned equivalently to the well-known Droop coefficients.

The derived dynamic equations and the resulting tuning method guarantee equivalent parallel active and reactive load power sharing, controlling the rate of change of the deduced frequency and voltage signals and their steady state values as well as being intuitive, easy to implement and representative of the physical meaning of each tunable value of the different controllers. However, the utilization and generalization of this approach in studying the limits of stability of the individual controllers needs further research.

References

1. Milano, F., Dörfler, F., Hug, G., Hill, D. J., & Verbič, G. (2018, June). Foundations and challenges of low-inertia systems. In *2018 power systems computation conference (PSCC)* (pp. 1-25). IEEE.
2. Guerrero, J. M., Chandorkar, M., Lee, T. L., & Loh, P. C. (2012). Advanced control architectures for intelligent microgrids—Part I: Decentralized and hierarchical control. *IEEE Transactions on Industrial Electronics, 60*(4), 1254-1262.
3. Rocabert, J., Luna, A., Blaabjerg, F., & Rodriguez, P. (2012). Control of power converters in AC microgrids. *IEEE transactions on power electronics, 27*(11), 4734-4749.
4. Han, Y., Li, H., Shen, P., Coelho, E. A. A., & Guerrero, J. M. (2016). Review of active and reactive power sharing strategies in hierarchical controlled microgrids. *IEEE Transactions on Power Electronics, 32*(3), 2427-2451.
5. Han, H., Hou, X., Yang, J., Wu, J., Su, M., & Guerrero, J. M. (2015). Review of power sharing control strategies for islanding operation of AC microgrids. *IEEE Transactions on Smart Grid, 7*(1), 200-215.
6. Tayyebi, A., Groß, D., Anta, A., Kupzog, F., & Dörfler, F. (2020). Frequency stability of synchronous machines and grid-forming power converters. *IEEE Journal of Emerging and Selected Topics in Power Electronics, 8*(2), 1004-1018.
7. U, M. Taouba. Jouini., and D, Groß. (2018).“MIGRATE Project – Deliverable 3.3: New options for existing system services and needs for new system services,” *Tech. Rep.*
8. Arghir, C., Jouini, T., & Dörfler, F. (2018). Grid-forming control for power converters based on matching of synchronous machines. *Automatica, 95*, 273-282.
9. Colombino, M., Groß, D., Brouillon, J. S., & Dörfler, F. (2019). Global phase and magnitude synchronization of coupled oscillators with application to the control of grid-forming power inverters. *IEEE Transactions on Automatic Control, 64*(11), 4496-4511.
10. X, K. Taoufik. Qoria., Quentin, Cossart., Chuanyue, Li., Xavier, Guillaud., Frederic, Colas., et al. (2018). “MIGRATE Project - Deliverable 3.2: Local control and simulation tools for large transmission systems,” MIGRATE Project, *Tech. Rep.*
11. Pogaku, N., Prodanovic, M., & Green, T. C. (2007). Modeling, analysis and testing of autonomous operation of an inverter-based microgrid. *IEEE Transactions on power electronics, 22*(2), 613-625.
12. Zhong, Q. C., & Weiss, G. (2010). Synchronverters: Inverters that mimic synchronous generators. *IEEE transactions on industrial electronics, 58*(4), 1259-1267.
13. Johnson, B., Rodriguez, M., Sinha, M., & Dhople, S. (2017, July). Comparison of virtual oscillator and droop control. In *2017 IEEE 18th Workshop on Control and Modeling for Power Electronics (COMPEL)* (pp. 1-6). IEEE.
14. Seo, G. S., Colombino, M., Subotic, I., Johnson, B., Groß, D., & Dörfler, F. (2019, March). Dispatchable virtual oscillator control for decentralized inverter-dominated power systems: Analysis and experiments. In *2019 IEEE Applied Power Electronics Conference and Exposition (APEC)* (pp. 561-566). IEEE.
15. Arghir, C., & Dörfler, F. (2019). The electronic realization of synchronous machines: Model matching, angle tracking, and energy shaping techniques. *IEEE Transactions on Power Electronics, 35*(4), 4398-4410.